

# Second-harmonic generation with focused beams under conditions of large group-velocity mismatch

Solomon M. Saltiel

*Faculty of Physics, University of Sofia, 5 J. Bourchier Boulevard, BG-1164, Sofia, Bulgaria*

Kaloian Koynov

*Max Planck Institute for Polymer Research, Ackermannweg 10, D-55128 Mainz, Germany*

Ben Agate and Wilson Sibbett

*School of Physics and Astronomy, University of St. Andrews, St. Andrews, KY16 9SS, Scotland*

Received July 10, 2003; revised September 29, 2003; accepted October 10, 2003

We present a theoretical model that describes the focusing conditions for second-harmonic generation (SHG) of focused femtosecond pulses as a function of group-velocity mismatch (GVM), with direct application to efficient SHG using a “thick” nonlinear crystal. We observe a direct dependence of the optimal focusing ratio,  $L/b$ , on the strength of group-velocity mismatch. Our model also describes the temporal duration of the second-harmonic pulses under these conditions as well as the change in optimal phase mismatch. The theoretical results are compared with an experiment for SHG with focused femtosecond pulses in a “thick” crystal of  $\text{KNbO}_3$ . © 2004 Optical Society of America

OCIS codes: 190.0190, 190.7110, 190.2620, 190.4360, 320.0320, 320.7110, 320.7080.

## 1. INTRODUCTION

The theoretical study of second-harmonic generation (SHG) using focused Gaussian beams by Boyd and Kleinman<sup>1</sup> has long been a reliable resource for those studying frequency-conversion processes. However, the Boyd–Kleinman theory applies only to cw beams and cannot be relied upon to describe harmonic generation correctly using ultrashort (femtosecond) pulses. In this paper, we provide a theoretical model that describes SHG using femtosecond pulses, by taking into account the associated critical effects of group-velocity mismatch (GVM). Our model explains successfully the experimentally observed behavior of SHG in the femtosecond regime,<sup>2,3</sup> in contrast to the somewhat inaccurate predictions of Boyd and Kleinman.

The efficiency of a parametric process is subject to limitations imposed by GVM, which describes a temporal walk-off between the interacting beams. This walk-off arises from a mismatch in the group velocities and becomes particularly significant in the ultrashort-pulse regime. Second-harmonic generation under conditions of large GVM is characterized by a nonstationary length,  $L_{\text{nst}}$ , defined by  $L_{\text{nst}} = \tau/\alpha$ , where  $\tau$  is the time duration of the fundamental pulses, and the GVM parameter,  $\alpha = 1/v_2 - 1/v_1$ , where  $v_2$  and  $v_1$  are the group velocities of the second-harmonic (SH) and fundamental waves, respectively. The nonstationary length,  $L_{\text{nst}}$ , is the distance at which two initially overlapped pulses at different wavelengths become separated by a time equal to  $\tau$ . In the ultrashort-pulse limit (i.e., for  $L_{\text{nst}} \ll L$ , where  $L$  is

the length of the nonlinear media) and for the case of an unfocused fundamental beam, the generated SH pulses are longer in time by a factor  $L/L_{\text{nst}}$ . In contrast to the well known quadratic dependence for the frequency doubling of cw waves, this process depends linearly on the length of the nonlinear media,  $L$ . As a result of this deleterious temporal broadening effect, nonlinear media are often chosen such that  $L \approx L_{\text{nst}}$ . However, while this may ensure generated SH pulses having durations close to that of the fundamental pulses, the interaction length is reduced, and the SHG efficiency is compromised.

The natural way to increase the efficiency of such a frequency-conversion processes is to use a focused fundamental beam. An established theory of SHG using focused cw beams<sup>1</sup> predicts, for negligible birefringence walk-off an optimal focusing condition that is expressed by the ratio  $L/b = 2.83$ , where  $b$  is the confocal parameter ( $b = k_1 w_{01}^2$ , where  $w_{01}$  and  $k_1$  are the focal spot radius and the wave vector of the fundamental wave, respectively). However, this theory applies only to the long-pulse or cw case, where GVM is negligible ( $L_{\text{nst}} \gg L$ ). We provide here, for the first time to our knowledge, a theoretical model that defines the optimum focusing conditions for SHG using focused beams in the ultrashort-pulse regime, where GVM is significant (i.e., where  $L \geq L_{\text{nst}}$ ).

Despite the limitations imposed on the length of the nonlinear media by the unwanted effects of GVM, several experimental papers on frequency doubling in  $\text{KNbO}_3$ ,<sup>2–6</sup>  $\text{LiB}_3\text{O}_5$ ,<sup>7</sup> and  $\beta$ -barium borate<sup>7</sup> have recently demon-

strated that efficient SHG is possible by focusing femtosecond (120–200-fs) pulses in “thick” nonlinear media, where the ratio  $L/L_{\text{nst}} > 20$ . These experiments have demonstrated that a conversion efficiency exceeding 60% is possible, and, as shown by Agate *et al.*,<sup>2</sup> the duration of the generated near-transform-limited SH pulses remained within the femtosecond regime, increasing only 2–3 times with respect to the fundamental duration. In these experiments, the optimal ratio  $L/b$  was found to be in the region of 10, which is far from the known Boyd and Kleinman ratio of  $L/b = 2.83$ . To our knowledge, no theoretical investigations exist that can predict the optimal focusing for SHG under conditions of large GVM. In the reported work of Weiner and Yu<sup>3,4</sup> a simple model is proposed that predicts well the efficiency of the SHG process, as well as identifying that an increase in SHG efficiency relates to an increase in the  $L/b$  ratio. Their model, however, does not predict the existence of optimal values for  $L/b$  and phase mismatch as obtained in both experiments discussed above. Also, it cannot describe the evolution of the SH temporal shape inside the crystal and does not give an optimal focusing position inside the nonlinear media.

In this paper, we present a theoretical model that describes the process of SHG under conditions of large GVM. This model assumes an undepleted fundamental beam and that both the fundamental and SH beam have Gaussian transverse distributions. The results of the model are compared with data from an SHG experiment using focused femtosecond pulses in a nonlinear crystal of potassium niobate (KNbO<sub>3</sub>).

## 2. THEORETICAL MODEL

Starting from Maxwell’s equations and using a slowly varying envelope approximation, we derive the following equations that describe the second-harmonic generation (SHG) of ultrashort pulses. The depletion of the fundamental beam, birefringence walk-off, and absorption losses for the both interacting waves are neglected.

$$\left( \frac{\partial}{\partial z} + \frac{i}{2k_1} \Delta_{\perp} + \frac{1}{v_1} \frac{\partial}{\partial t} \right) A_1 = 0, \quad (1)$$

$$\left( \frac{\partial}{\partial z} + \frac{i}{2k_2} \Delta_{\perp} + \frac{1}{v_2} \frac{\partial}{\partial t} \right) A_2 = -i\sigma_2 A_1^2 \exp(i\Delta kz), \quad (2)$$

where  $A_1$  and  $A_2$  denote the complex amplitudes of the fundamental and the second-harmonic waves, respectively, and are functions of three spatial coordinates and one temporal coordinate,  $A_j = A_j(x, y, z, t)$ .  $\Delta_{\perp}$  stands for the operator

$$\frac{\partial^2}{\partial x^2} + \frac{\partial^2}{\partial y^2}.$$

The nonlinear coupling coefficient,  $\sigma_2$ , is calculated as  $\sigma_2 = 2\pi d_{\text{eff,SHG}}/(\lambda_1 n_2)$ , where the magnitude of  $d_{\text{eff,SHG}}$  depends on the method of phase matching and the type of the nonlinear medium that is used. The wave-vector mismatch is defined as  $\Delta k = k_2 - 2k_1$ , where  $k_1$  and  $k_2$  are the wave vectors of the two waves, respectively.

System (1) and (2) is solved by the trial-solution method as described in Ref. 8. Let us assume that the input fundamental has a Gaussian spatial distribution. Assuming also that the fundamental beam experiences no depletion, its transverse distribution will remain Gaussian throughout the entire interaction. Therefore we can accept

$$A_1(x, y, z, t) = A(z, t)g_1(x, y, u_1), \quad (3)$$

with

$$g_1(x, y, u_1) = \frac{1}{1 - iu_1} \exp\left[-\frac{x^2 + y^2}{w_{01}^2(1 - iu_1)}\right],$$

$$u_1 = 2z/b_1.$$

The polarization inside the nonlinear media, described by the right side of Eq. (2), will have a Gaussian spatial distribution and leads to the generated SH beam having the same transverse distribution:

$$A_2(x, y, z, t) = S(z, t)g_2(x, y, u_2), \quad (4)$$

with

$$g_2(x, y, u_2) = \frac{1}{1 - iu_2} \exp\left[-\frac{x^2 + y^2}{w_{02}^2(1 - iu_2)}\right],$$

$$u_2 = 2z/b_2.$$

These conditions have been assumed by several authors,<sup>8–10</sup> where the aim was to find the optimal focusing conditions for nonlinear interactions with cw or quasi-cw beams. As shown in Refs. 8 and 9,  $w_{02} = w_{01}/\sqrt{2}$ , and consequently  $b_2 \approx b_1$ , which leads to

$$u_2 = u_1 = u = 2z/b.$$

Substituting Eq. (3) and Eq. (4) into Eq. (1) and Eq. (2) and taking into account that

$$\left[ \frac{\partial g_j}{\partial z} + \frac{i}{2k_1} \Delta_{\perp} g_j \right] \equiv 0 \quad (j = 1, 2),$$

we get

$$\frac{\partial A(z, t)}{\partial z} + \frac{1}{v_1} \frac{\partial A(z, t)}{\partial t} A = 0, \quad (5)$$

$$\frac{\partial S(z, t)}{\partial z} + \frac{1}{v_2} \frac{\partial S(z, t)}{\partial t} = -i\sigma_2 A(z, t)^2 \frac{(g_1)^2}{g_2} \exp(i\Delta kz). \quad (6)$$

With the standard substitution  $q = t - z/v_1$ , Eq. (5) transforms into  $[\partial A(z, q)]/\partial z = 0$ , giving that  $A(z, q) = A(q)$ . From Eq. (3) and Eq. (4),  $g_1^2/g_2 = 1/(1 - iu)$ , and therefore Eq. (6) becomes

$$\frac{\partial S(z, q)}{\partial z} + \alpha \frac{\partial S(z, q)}{\partial q} = \frac{-i\sigma_2}{1 - iu} A(q)^2 \exp(i\nu u), \quad (7)$$

where

$$\nu = \frac{\Delta kb}{2} = \frac{\Delta kL}{2m}, \quad m = \frac{L}{b}.$$

It is important to note that  $A(q)$  and  $S(z, q)$  represent the recalculated field amplitudes at the center of the

beam and at the position of the focal spot ( $x = 0, y = 0, z = 0$ ).

Assuming no SH signal at the input of the nonlinear crystal, the solution of Eq. (7) is

$$S(L, p) = -i\sigma_2 A_0^2 b H_{\text{tr}}(m, \mu, \nu, \gamma, p), \quad (8)$$

with

$$H_{\text{tr}}(m, \mu, \nu, \gamma, p) = \frac{1}{2} \int_{-m(1+\mu)}^{m(1-\mu)} \frac{du}{1-iu} T \times \left[ T \left( \frac{p}{\tau} + \gamma u \right) \right]^2 \exp(i\nu u), \quad (9)$$

where  $p$  is the local time attached to the time position of the SH pulse,  $p = q - z\alpha = t - z/v_2$ .

In Eq. (9) with function  $T(t/\tau)$ , we denote the temporal shape of the fundamental-pulse amplitude normalized to 1. Also

$$\gamma = \frac{\alpha b}{2\tau} = \frac{1}{2m} \frac{L}{L_{\text{nst}}},$$

and  $\mu$  indicates the position of the focus spot inside the crystal;  $\mu = 0$  corresponds to the center of the crystal;  $\mu = -1$  is the focus is at the input face; and  $\mu = +1$  is the focus is at the output face.

In the limit of  $m \ll 1$ , i.e., the weak focusing limit of  $b \gg L$ , Eq. (8) reduces to

$$S(L, t) = -i\sigma_2 A_0^2 L \int_{-1/2}^{1/2} \left[ T \left( \frac{t - z/v_2 + \alpha Lx}{\tau} \right) \right]^2 \times \exp(i\Delta k Lx) dx, \quad (10)$$

which is the well-known expression for nonstationary doubling in a plane-wave approximation.<sup>11–14</sup>

Taking into account that the intensity of the SH beam at the output of the crystal is  $I_{\text{sh}}(L, p) = (c\epsilon_0 n_2/2) |A_2(x, y, L, p)|^2$ , the energy of the SH pulse,  $W_{\text{sh}}(L)$ , can then be found by integrating the SH intensity  $I_{\text{sh}}(L, p)$  over space and time:

$$W_{\text{sh}}(L) = \frac{1}{8} \pi w_{01}^2 (c\epsilon_0 n_2) \sigma_2^2 b^2 |A_0|^4 \tau \times \int_{-\infty}^{+\infty} |H_{\text{tr}}(m, \mu, \nu, \gamma, p)|^2 dp. \quad (11)$$

To find the conversion efficiency in a suitable form for calculation, we assume a hyperbolic secant temporal shape [ $T(t/\tau) = \text{sech}(t/\tau)$ ] for the fundamental pulses, and by using  $|A_0|^2 = 4W_{\text{fund}}/(b\lambda\tau\epsilon_0)$  here, we obtain

$$\frac{W_{\text{sh}}}{W_{\text{fund}}} = K h_{\text{tr}}(m, \mu, \nu, \gamma), \quad (12)$$

with

$$K = \frac{4\sigma_2^2 n_2 L}{\lambda_1 c \epsilon_0 n_1} \frac{W_{\text{fund}}}{3\tau} = \frac{16\pi^2 d_{\text{eff}}^2 W_{\text{fund}} L}{3\lambda_1^3 c \epsilon_0 n_2 n_1 \alpha L_{\text{nst}}},$$

$$h_{\text{tr}}(m, \mu, \nu, \gamma) = \frac{3}{4m} \int_{-\infty}^{+\infty} |H_{\text{tr}}(m, \mu, \nu, \gamma, p')|^2 dp'. \quad (13)$$

where  $W_{\text{sh}}/W_{\text{fund}}$  is the ratio of second harmonic to fundamental-pulse energy (SHG efficiency),  $K$  is a constant,  $h_{\text{tr}}(m, \mu, \nu, \gamma)$  is a transient focusing factor, and  $p' = p/\tau$ .

### 3. NUMERICAL RESULTS

The dependence of the SH efficiency on the main parameters—strength of focusing,  $m = L/b$ , temporal walk-off distance,  $L_{\text{nst}}$ , phase mismatch,  $\Delta k$ , and position of focusing,  $\mu$ —is given by the transient focusing factor,  $h_{\text{tr}}$ . The SHG efficiency,  $\eta$ , can be found by multiplying the value of  $h_{\text{tr}}$  to the constant  $K$ . The SHG slope efficiency (or normalized SHG efficiency) we use below is given by  $\eta_{\text{slope}} = K h_{\text{tr}}/W_{\text{fund}}$ . In order to obtain the maximum frequency-doubling efficiency, three parameters must be optimized: (i) the phase mismatch,  $\Delta k$ ; (ii) the position of the focal spot,  $\mu$ ; and (iii) the strength of focusing,  $m = L/b$ .

Just as in the process of SHG with focused cw beams, the maximum SH signal for SHG with focused ultrashort pulses is obtained for some optimized deviation from ex-

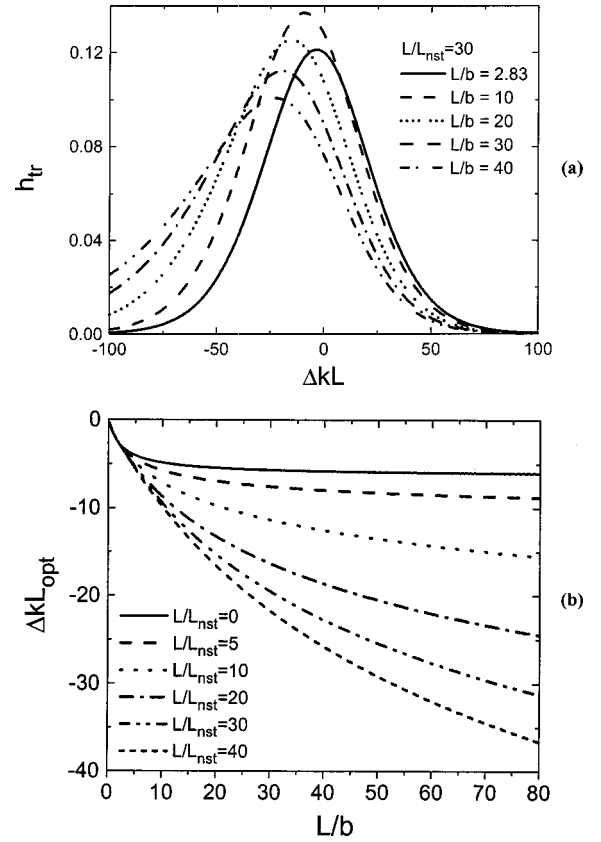


Fig. 1. (a) Value of transient focusing factor,  $h_{\text{tr}}$ , as a function of normalized phase mismatch,  $\Delta kL$ , for different focusing strengths of  $m = L/b$ . The temporal walk-off parameter  $L/L_{\text{nst}} = 30$ . (b) The optimal values of normalized phase mismatch,  $\Delta kL_{\text{opt}}$ , as a function of  $m$  for different values of  $L/L_{\text{nst}}$ . For both (a) and (b), the fundamental focal spot is in the center of the nonlinear media  $\mu = 0$ .

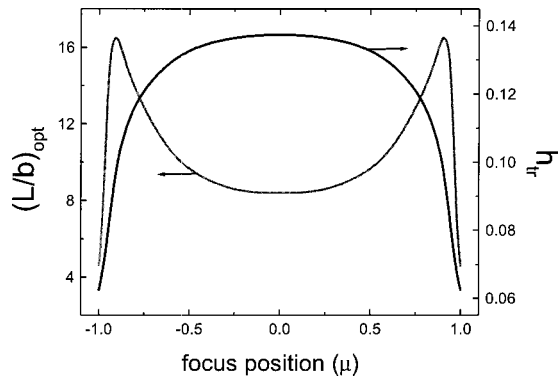


Fig. 2. Dependence of the transient focusing factor,  $h_{tr}$ , and optimal focusing,  $m_{opt} = (L/b)_{opt}$ , on the position,  $\mu$ , of the fundamental focal spot inside the nonlinear media. Data are calculated for  $\Delta kL = \Delta kL_{opt}$  and  $L/L_{nst} = 30$ .

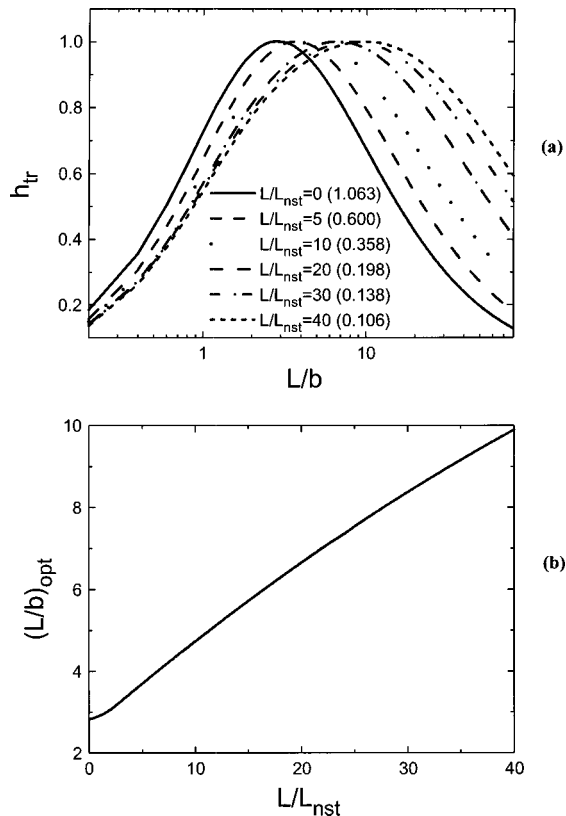


Fig. 3. (a) Dependence of the transient focusing factor,  $h_{tr}$ , on focusing strength,  $m$ , for different values of the temporal walk-off parameter,  $L/L_{nst}$ . Each curve is normalized to its own maximum; the absolute values of each maxima are shown in brackets. (b) Dependence of optimal focusing strength,  $m_{opt} = (L/b)_{opt}$ , on  $L/L_{nst}$ . Focal position lies in the center of the nonlinear medium ( $\mu = 0$ ) and  $\Delta kL = (\Delta kL)_{opt}$ .

act phase-matching conditions. In Fig. 1(a), we present the calculated phase-matching tuning curves as a function of  $\Delta kL$ : the normalized detuning from exact phase matching, for various focusing strengths ( $m = 2.83, 10, 20, 30$ , and  $40$ ) in a thick nonlinear crystal (we use the example  $L/L_{nst} = 30$ ). It can be seen that with stronger focusing, a larger deviation is required from exact phase matching. It should also be noted that the tuning curves

have no side lobes or secondary maxima in contrast to the typical  $\text{sinc}^2$  response for experiments with weak or no focusing. The values of the optimal normalized phase mismatches  $(\Delta kL)_{opt}$  under different focusing strengths are shown in Fig. 1(b) for various values of the temporal walk-off parameter,  $L/L_{nst}$ .

In Fig. 2, we plot the transient focusing factor,  $h_{tr}$ , (which is proportional to SH energy and SHG efficiency) as a function of the focal position,  $\mu$ , which indicates that the optimum position for the focused spot waist is at the center of the nonlinear crystal ( $\mu = 0$ ). We also plot the optimal focusing strength,  $m_{opt} = (L/b)_{opt}$ , as a function of  $\mu$ . We see that off-center focusing ( $\mu \neq 0$ ) leads to different optimized conditions (i.e., strongest focusing) at the edges of the nonlinear crystal. The remaining figures below are all plotted with optimized mismatch  $\Delta kL = (\Delta kL)_{opt}$  and for focusing in the center of the nonlinear crystal.

Figure 3(a) illustrates the dependence of the value of the transient focusing factor,  $h_{tr}$ , on the focusing parameter,  $m$ , for different values of the temporal walk-off parameter,  $L/L_{nst}$ . Each curve is normalized to its maximum; absolute values of each maxima are shown in brackets. It can be seen that for each value of  $L/L_{nst}$  an optimal focusing strength exists. Therefore for the SHG of ultrashort pulses, the optimal focusing strength,  $m_{opt} = (L/b)_{opt}$ , for any given temporal walk-off parameter,  $L/L_{nst}$ , can be obtained from Fig. 3(b). In the limit of  $L/L_{nst} \rightarrow 0$ , the optimal ratio of  $L/b$  approaches the well-known Boyd–Kleinman<sup>1</sup> value of 2.83 for SHG in the cw regime. Figure 3 concerns the optimization of focusing strength for obtaining the maximum SH pulse energy. As we discuss below [Fig. 6(b)], the optimum focusing strength is different when maximizing the SH pulse peak intensity.

The dependence of the transient focusing factor,  $h_{tr}$ , on the temporal walk-off parameter,  $L/L_{nst}$ , for different focusing strengths is shown in Fig. 4. The value of  $h_{tr}$  monotonically decreases with an increase in  $L/L_{nst}$ . For  $L_{nst} \ll b$ , the dependence of the SH efficiency becomes  $\eta \propto (L/L_{nst})^{-1}$ , in accordance with the prediction of the previously published model.<sup>3,4</sup>

In Fig. 5(a), we demonstrate that, under conditions of strong focusing, the SH pulse duration,  $\tau_{SH}$ , remains

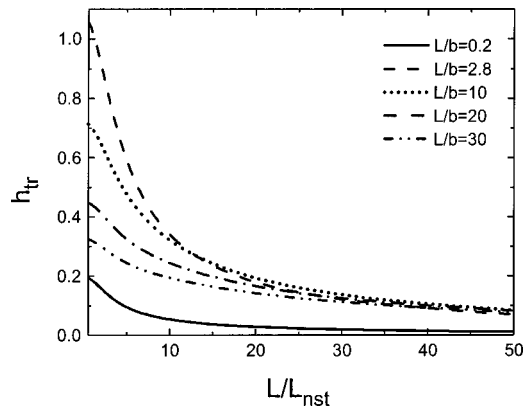


Fig. 4. Transient focusing factor,  $h_{tr}$ , as a function of the temporal walk-off parameter,  $L/L_{nst}$ , for different focusing strengths,  $m = L/b$ . Focal position  $\mu = 0$  and  $\Delta kL = \Delta kL_{opt}$ .

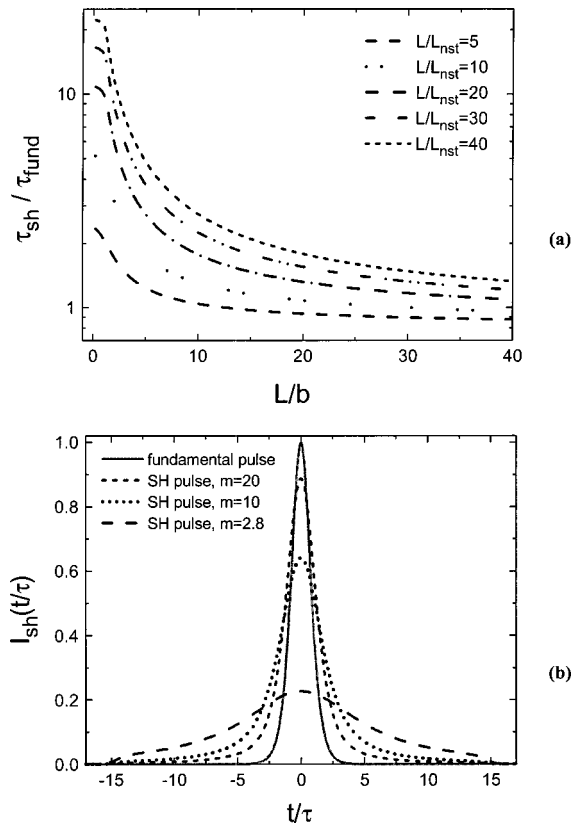


Fig. 5. (a) Ratio of the output SH pulse duration to the fundamental pulse duration as a function of the focusing strength,  $m = L/b$ , and different values of  $L/L_{nst}$ . (b) Temporal profiles and relative intensities of the generated SH pulses calculated for several values of  $m$  at  $L/L_{nst} = 30$ . The fundamental pulse,  $T(t/\tau)$ , is shown for comparison. The SH pulses correspond to  $(75/4m)|H_{tr}(t/\tau)|^2$ . Focal position  $\mu = 0$  and  $\Delta kL = (\Delta kL)_{opt}$ .

close to the initial fundamental-pulse duration,  $\tau_{fund}$ , even at large values of  $L/L_{nst}$ . The reason for this is that the region where the process of SHG is efficient is defined by the magnitude of the confocal parameter,  $b$ . The amount of temporal broadening of the SH pulse with respect to the fundamental pulse can therefore be estimated from Fig. 5(a) using the known ratio of  $L/L_{nst}$  and strength of focusing,  $m = L/b$ . By simply selecting the appropriate focusing lens, it is therefore possible to control the duration of the generated SH pulse. Although a lengthening of the SH pulse is accompanied by some frequency chirp, additional analysis has revealed that this chirp is not linear, and therefore compression of the SH pulses by conventional methods is not possible. The temporal pulse shapes presented in Fig. 5(b) confirm that stronger focusing results in shorter SH pulse durations. The peak intensity ( $\propto W_{SH}/\tau_{SH}$ ) of the SH pulse obtained with strong focusing of  $L/b = 20$  is more than four times higher than the SH pulse obtained with the Boyd-Kleinman optimum of  $L/b = 2.8$ .

To confirm this and to illustrate the advantage of the “thick” crystal approach for frequency doubling of femto-second pulses, we plot in Fig. 6(a) the SHG efficiency,  $\eta$ , and SH pulse duration,  $\tau_{SH}$ , for a “thick” nonlinear crystal of length  $L = ML_{nst}$ . The values of  $\eta$  and  $\tau_{SH}$  are

normalized to their respective values for a conventional “thin” crystal of length  $L = L_{nst}$ . As calculated earlier using our model, the duration of a SH pulse generated in a “thin” crystal (with  $L = L_{nst}$ ) is 1.3 times that of the fundamental pulse. The clear advantage of the thick crystal approach is demonstrated in Fig. 6(a), where the SHG efficiency is increased by a factor of 4 ( $\eta_{SH}/\eta_{SH,L=L_{nst}} = 4.3$  for  $L/L_{nst} = 40$ ). At the same time, the SH pulse duration is lengthened only by a few times with respect to the fundamental pulse, depending on the value of  $L/L_{nst}$  ( $\tau_{SH}/\tau_{SH,L=L_{nst}} \sim 3.75$  for  $L/L_{nst} = 40$ ).

In some applications, it is important for the generated SH pulse to be optimized for maximum peak intensity,  $I_{peak,sh} = W_{sh}/\tau_{sh}$ . This is the case, for example, when the output second-harmonic pulse is involved in another nonlinear process such as fourth-harmonic generation in an additional nonlinear crystal. In Fig. 3(a), we identified the optimum focusing conditions for obtaining the maximum SH pulse energy. In Fig. 6(b), we now plot the quantity  $h_{tr}/\tau_{SH}$  (which is proportional to the SH pulse

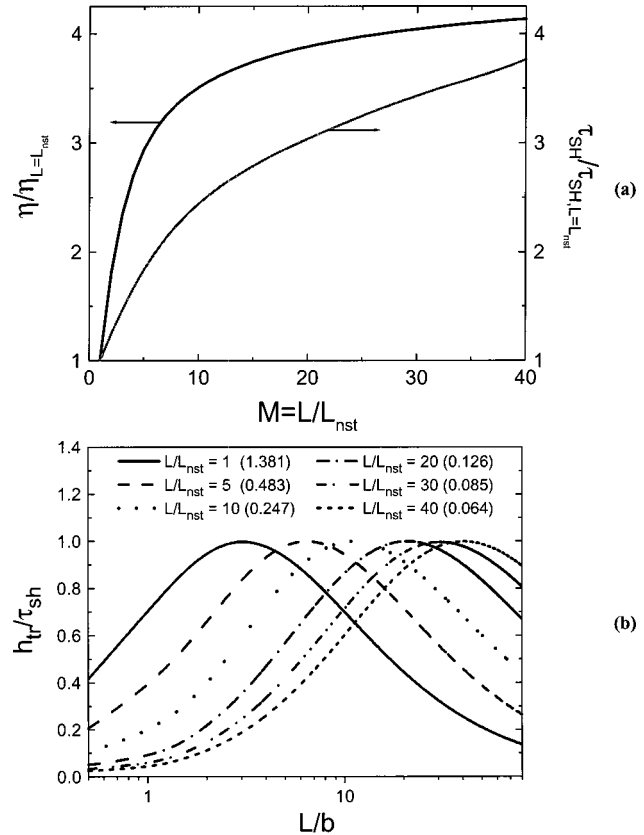


Fig. 6. (a) Advantage of using a “thick” crystal with respect to a “thin” crystal. Left scale: Relative increase in SHG efficiency,  $\eta_{SH}/\eta_{SH,L=L_{nst}}$ , as a function of increasing crystal thickness,  $L/L_{nst}$ . A typical “thin” crystal is defined as  $L = L_{nst}$ . Right scale: Relative increase in SH pulse duration,  $\tau_{SH}/\tau_{SH,L=L_{nst}}$ , as a function of increasing  $L/L_{nst}$ . Data are calculated at  $\Delta kL = (\Delta kL)_{opt}$  and  $L/b = (L/b)_{opt}$ . The values of  $(L/b)_{opt}$  are shown in Fig. 3(b). (b) Dependence of the quantity  $h_{tr}/\tau_{SH}$  on focusing strength,  $L/b$ , for different values of  $L/L_{nst}$ . (See the text for more details). Each curve is normalized to its own maximum; the absolute values of the maxima are shown in brackets. Focal position  $\mu = 0$  and  $\Delta kL = (\Delta kL)_{opt}$ .

peak intensity) as a function of the focusing parameter  $m = L/b$  for different values of  $L/L_{\text{nst}}$ . Comparing the case of  $L/L_{\text{nst}} = 30$  with Fig. 3(a) [ $(L/b)_{\text{opt,energy}} \sim 10$ ], we see that the maximum SH pulse peak intensity from Fig. 6(b) requires three times the strength of focusing [ $(L/b)_{\text{opt,power}} \sim 30$ ]. We also note that the optimal focusing for maximum SH pulse peak intensity for any given crystal length,  $L$ , is satisfied when  $L_{\text{nst}} \approx b$ .

#### 4. COMPARISON WITH EXPERIMENT

Experimental assessments<sup>2</sup> were performed with a compact Cr:LiSAF femtosecond laser<sup>15</sup> that provided pulses with a full-width at half maximum (FWHM) of 210 fs ( $\pm 10\%$ ), an average power of up to 45 mW and a pulse repetition rate of 330 MHz at  $\lambda_{\text{fund}} = 860$  nm. In order to calculate  $L_{\text{nst}} = \tau/\alpha$ , we have assumed a fundamental pulse with a hyperbolic secant temporal profile, and therefore  $\tau = \tau_{\text{fund}}(\text{FWHM})/1.76$ . The femtosecond pulses were tightly focused into a 3-mm length of bulk potassium niobate (KNbO<sub>3</sub>), which was tuned for the process of type I noncritical phase matching. The maximum optical-to-optical SHG efficiency achieved was 30%. The corresponding value of  $L/L_{\text{nst}}$  under these conditions ( $\alpha_{\text{KNbO}_3} = 1.2$  ps/mm) is  $L/L_{\text{nst}} = 30$ . The values of beam waist,  $w_{01}$ , and confocal parameter,  $b$ , are calculated from conventional *ABCD* matrices using the measured beam diameter,  $d$ , before the focusing lens. The experimental uncertainties in the determination of  $w_{01}$  and  $b$  are 5% and 10%, respectively.

In Fig. 7(a), we show the experimental values of normalized SHG efficiency as a function of the focusing strength,  $m = L/b$ . The experimental data are plotted together with theoretical predictions from our model described here, as well as the model published in Refs. 3 and 4. Both models assume the ratio  $L/L_{\text{nst}} = 30$ , and both theoretical curves are normalized for  $L/b = 10$ . We see from Fig. 7(a) that our model describes correctly the existence of a maximum in the dependence of SHG efficiency on focusing strength. To determine whether our model predicts the absolute efficiency, we have made use of the initial part ( $< 20\%$ ) of the experimental data (published in Ref. 2). Working with different published values for the second-order nonlinearity constant,  $d_{32}$ , of KNbO<sub>3</sub>,<sup>16–18</sup> we find that the corrected value of  $d_{32} = 12.5$  pm/V published in Ref. 18 gives the best agreement not only with the experiment reported here, but also with the experimental work published previously.<sup>3,4</sup> In Table 1, we compare the slope efficiency achieved in the experiment with the predicted from our model and that presented

earlier.<sup>3,4</sup> The experimentally observed temporal broadening of the SH pulse ( $\tau_{\text{SH}}/\tau_{\text{fund}}$ ) is also compared with the prediction of our model.

We consider the agreement between experiment and theory for the slope efficiency,  $\eta_{\text{slope}}$ , to be very good, taking into account that the theoretical values are calculated from experimental values of  $\tau_{\text{fund}}$  and  $b$ , which have a 10% error margin. The agreement for the lengthening of the SH pulse,  $\tau_{\text{SH}}/\tau_{\text{fund}}$ , is also excellent. At this point, we would like to note that the model described in Refs. 3 and 4 cannot explain the change in SH pulse durations. This

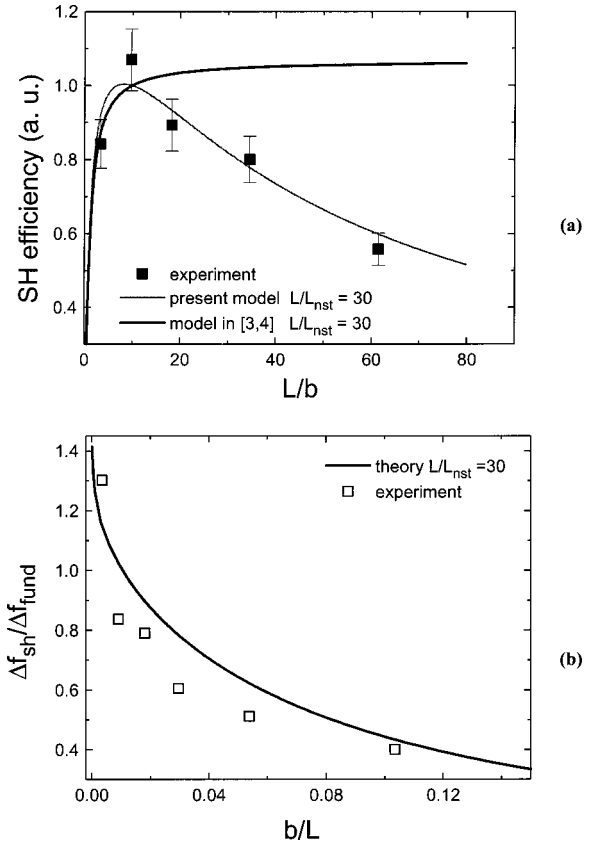


Fig. 7. (a) Experimental values of SHG efficiency (data points), and the predictions of our model (gray curve) and another model<sup>3,4</sup> (black curve) for  $L/L_{\text{nst}} = 30$ , as a function of the focusing strength  $m = L/b$ . The two theoretical curves are normalized to their values for  $L/b = 10$ , which was the observed optimal focusing strength in the experiment.<sup>2</sup> The maximum experimental point corresponds to a SHG efficiency of 30%. (b) Experimentally measured evolution of the SH pulse spectral width relative to the fundamental spectral width (data points), and the theoretical prediction of our model calculated for  $L/L_{\text{nst}} = 30$ , as a function of the ratio  $b/L$ . The curves that represent our model are for focal position  $\mu = 0$  and  $\Delta kL = (\Delta kL)_{\text{opt}}$ .

**Table 1. Comparison of the Predictions of Our Model with the Experiment in KNbO<sub>3</sub>,<sup>2</sup> and the Predictions of Other Models<sup>3,4a</sup>**

$W_{\text{fund}}$	$\tau_{\text{fund}}$	$L$	$\eta_{\text{slope}}$ (Experiment)	$\eta_{\text{slope}}$ (Our Model)	$\eta_{\text{slope}}$ (Model <sup>3,4</sup> )	$\tau_{\text{SH}}/\tau_{\text{fund}}$ (Experiment)	$\tau_{\text{SH}}/\tau_{\text{fund}}$ (Our Model)
$< 70$ pJ	210 fs	3 mm	0.25%/pJ	0.32%/pJ	0.34%/pJ	2.6	2.4

<sup>a</sup>  $W_{\text{fund}}$  is the fundamental-pulse energy;  $\tau_{\text{fund}}$  is the fundamental-pulse duration;  $L$  is the nonlinear media length;  $\eta_{\text{slope}}$  is the SHG slope efficiency;  $\tau_{\text{SH}}/\tau_{\text{fund}}$  is the ratio of SH to fundamental-pulse durations.

is because this model is built on the restricting assumptions of unchanging pulse shapes and constant duration for both interacting waves.

Experimentally, it was not possible to measure the dependence of the SH pulse duration on focusing strength due to the low sensitivity of the pulse-duration measurement system. Instead, the dependence of the SH pulse spectral width was measured as a function of focusing strength. In Fig. 7(b), the experimentally measured narrowing of the SH spectral width with an increase of ratio  $b/L$  is compared with the theoretical prediction from our model. To plot the theoretical curve in Fig. 7(b), we have assumed transform-limited pulses with a temporal profile given by  $\Delta f_{\text{fund}}/\Delta f_{\text{sh}} = \tau_{\text{sh}}/\tau_{\text{fund}}$ . An increase in the confocal parameter,  $b$ , leads to an exaggerated presence of GVM. The SH pulses therefore become longer, and the spectral width therefore decreases. On the other hand, for very small values of the confocal parameter,  $b$ , the SHG process is stationary, and the transformation of the spectra behaves as if in the long-pulse limit. We can see that the model presented here also describes the spectra of the generated SH pulses, although the presumption that the SH pulses have a hyperbolic secant temporal profile is quite approximate. Correct accounting of the SH pulse shape would improve the accuracy of the model even further. Significantly, the model reported in Refs. 3 and 4 is not able to describe such a dependence for the reasons discussed above. Although our analysis has assumed fundamental pulses with no frequency chirp, it is possible to extend the present model to describe SHG with chirped fundamental pulses.

In another study of SHG in the femtosecond regime, an experiment to determine the optimal focal position within a bulk  $\text{KNbO}_3$  crystal has been carried out.<sup>5</sup> It was shown that, at low powers below the saturation regime, the optimal position of the focal spot is indeed in the center of the crystals, as predicted by our present model.

## 5. CONCLUSION

In conclusion, we have presented a model that extends the well-known Boyd–Kleinman theory to take account of the temporal walk-off effects of group-velocity mismatch in the SHG of ultrashort pulses using focused beams. We have verified the model using results from a frequency-doubling experiment involving a  $\text{KNbO}_3$  nonlinear crystal. The model described here is suitable for cases when birefringence walk-off can be neglected, such as SHG with noncritical phase matching and SHG in a quasi-phase-matched structure.<sup>19</sup> The model, which assumes negligible depletion of the fundamental, provides information on the efficiency of the SHG process, the pulse duration of the SH pulses, and the modification of the phase-matching tuning curves. In addition, it allows for optimization of the SHG process by selecting the optimal phase mismatch, focusing strength and position of focusing within the nonlinear medium. We believe that the model can be extended to describe the following:

- Other quadratic and cubic processes such as sum- and difference-frequency mixing, and third and fourth (and higher) harmonic generation.

- SHG with Gaussian and other fundamental temporal pulse shapes.
- SHG with chirped fundamental pulses.

We are confident that this model will be an efficient tool in the design of femtosecond SHG schemes with predictable parameters. (Part of this work has been presented as a poster at a recent conference<sup>20</sup>).

## ACKNOWLEDGMENTS

S. Sattiel and K. Koynov thank the Bulgarian Ministry of Science and Education for the support with Science Fund grant F-1201/2002. K. Koynov acknowledges also the support through a European Community Marie Curie Fellowship.

## REFERENCES

1. G. D. Boyd and D. A. Kleinman, "Parametric interactions of focused Gaussian light beams," *J. Appl. Phys.* **39**, 3897–3641 (1968).
2. B. Agate, A. J. Kemp, C. T. A. Brown, and W. Sibbett, "Efficient, high repetition-rate femtosecond blue source using a compact Cr:LiSAF laser," *Opt. Express* **10**, 824–831 (2002).
3. A. M. Weiner, A. M. Kan'an, and D. E. Leaird, "High-efficiency blue generation by frequency doubling of femtosecond pulses in a thick nonlinear crystal," *Opt. Lett.* **23**, 1441–1443 (1998).
4. S. Yu and A. M. Weiner, "Phase-matching temperature shifts in blue generation by frequency doubling of femtosecond pulses in  $\text{KNbO}_3$ ," *J. Opt. Soc. Am. B* **16**, 1300–1304 (1999).
5. D. Guzun, Y. Q. Li, and M. Xiao, "Blue light generation in single-pass frequency doubling of femtosecond pulses in  $\text{KNbO}_3$ ," *Opt. Commun.* **180**, 367–371 (2000).
6. Y. Q. Li, D. Guzun, G. Salamo, and M. Xiao, "High-efficiency blue-light generation by frequency doubling of picosecond pulses in a thick  $\text{KNbO}_3$  crystal," *J. Opt. Soc. Am. B* **20**, 1285–1289 (2003).
7. H. Wang and A. M. Weiner, "Second harmonic generation efficiency with simultaneous temporal walkoff, spatial walkoff, and depletion," *Conference on Lasers and Electro-Optics*, Vol. 89 of Trends in Optics and Photonics Series (Optical Society of America, Washington, D.C., 2003), paper CThU1.
8. R. W. Boyd, *Nonlinear Optics* (Academic, New York, 1992) Chap. II, p. 94.
9. V. Magni, "Optimum beams for efficient frequency mixing in crystals with second order nonlinearity," *Opt. Commun.* **184**, 245–255 (2000).
10. G. D. Xu, T. W. Ren, Y. H. Wang, Y. Y. Zhu, S. N. Zhu, and N. B. Ming, "Third-harmonic generation by use of focused Gaussian beams in an optical superlattice," *J. Opt. Soc. Am. B* **20**, 360–365 (2003).
11. S. A. Akhmanov, V. A. Vysloukh, and A. S. Chirkin *Optics of Femtosecond Laser Pulses* (American Institute of Physics, New York, 1992), Chap. 3, p. 141.
12. E. Sidick, A. Knoesen, and A. Dienes, "Ultrashort pulse second-harmonic generation in quasi-phase-matched dispersive media," *Opt. Lett.* **19**, 266–268 (1994).
13. E. Sidick, A. Knoesen, and A. Dienes, "Ultrashort-pulse second-harmonic generation. I. Transform-limited fundamental pulses," *J. Opt. Soc. Am. B* **12**, 1704–1712 (1995).
14. J. T. Manassah and O. R. Cockings, "Induced phase modulation of a generated second-harmonic signal," *Opt. Lett.* **12**, 1005–1007 (1987).

15. B. Agate, B. Stormont, A. J. Kemp, C. T. A. Brown, U. Keller, and W. Sibbett, "Simplified cavity designs for efficient and compact femtosecond Cr:LiSAF lasers," *Opt. Commun.* **205**, 207–213 (2002).
16. G. G. Gurzadian, V. G. Dmitriev, and D. N. Nikogosian, *Handbook of Nonlinear Optical Crystals*, 3rd ed., Vol. 64 of Springer Series in Optical Sciences (Springer-Verlag, New York, 1999).
17. I. Biaggio, P. Kerkoc, L.-S. Wu, P. Günter, and B. Zysset, "Refractive indices of orthorhombic  $\text{KNbO}_3$ . II. Phase matching configurations for nonlinear-optical interactions," *J. Opt. Soc. Am. B* **9**, 507–517 (1992).
18. I. Shoji, T. Kondo, A. Kitamoto, M. Shirane, and R. Ito, "Absolute scale of second-order nonlinear-optical coefficients," *J. Opt. Soc. Am. B* **14**, 2268–2294 (1997).
19. M. M. Fejer, G. A. Magel, D. H. Jundt, and R. L. Byer, "Quasi-phase matched second harmonic generation: tuning and tolerances," *IEEE J. Quantum Electron.* **28**, 2631–2654 (1992).
20. S. M. Saltiel, K. Koynov, B. Agate, and W. Sibbett, "Second harmonic generation with focused beams under conditions of large group velocity mismatch," presented at the Eleventh Conference on Laser Optics (LO'2003), St. Petersburg, Russia, June 30–July 04, 2003, Poster WeR1-39p.